Exploring the potentials of lean-burn hydrogen SI engine compared to methane operation.

Paolo Sementa[a], Jácson Beltrão de Vargas Antolini[b], Cinzia Tornatore[a*], Francesco Catapano[a], Bianca Maria Vaglieco[a] and José Javier López Sánchez[b]

[a] STEMS-CNR: Institute of Science and Technology for Sustainable Energy and Mobility, Italian National Research Council, via Marconi, 4, 80125 Napoli (Italia)

[b] CMT - Motores Térmicos, Universitat Politècnica de València, Edificio 6D, Camino de Vera, s/n, 46022 Valencia (España)

Corresponding author (*): Cinzia Tornatore, cinzia.tornatore@stems.cnr.it

Abstract

The global rush for decarbonization and the more restrictive emission regulations are pushing the research for cleaner powertrains to the transport sector. In this sense, this work contributes with an experimental investigation of the performance and emissions of a single-cylinder SI engine operating under lean-burn hydrogen combustion. Its performance, combustion parameters, exhaust emissions, and indicated efficiency for a wide range of mixture dilutions are then compared to methane under similar engine load conditions. Hydrogen achieved stable combustion up to lambda 3.4, presenting zero CO emission and very low HC emission for all tested operating conditions. Hydrogen operation also presented zero NOx emissions for conditions leaner than lambda 2.2 and 3.0 at 2000 and 3000 rpm, respectively, however, the NOx emissions increase as the mixture is enriched. The high in-cylinder pressure rise rate limited the operation at mixtures richer than lambda 1.3 at 2000 rpm. When compared to methane, the hydrogen allows de-throttle the engine to burn lean mixtures maintaining a proper flame speed, resulting in lower pumping losses, lower pollutants emissions for most of the conditions tested, and higher indicated efficiency, making hydrogen a promising fuel to replace conventional fuels on cleaner SI engines.

Keywords

Hydrogen fuel; SI engine; lean combustion; methane.

1. Introduction

The imperative shift towards a cleaner energy infrastructure pushed by the concern about global warming and air pollution in big cities is driving the policy makers to impose emission regulations more and more restrictive to commercial and passenger cars [1,2]. These restrictions have led to several improvements in terms of fuel conversion efficiency and tailpipe emission reduction over the last years [3,4]. The upcoming regulations in the transport sector are directing attention mainly to the powertrain electrification, but more efficient Well-to-Wheel (WTW) solutions as the use of alternative fuels on the already widespread internal combustion engine (ICE) or the use of unconventional technologies such as fuel cell has also been studied [5].

One of the most promising fuels to extend the use of ICE in transportation is the hydrogen, a carbon-free fuel that can be produced from renewable energy sources and which produces zero carbon emission from its combustion, aside from the nitrogen oxides formed due to the high-temperature combustion [6–8]. Like all gaseous fuels, the hydrogen has the drawback of low energy density, requiring a larger (and at high pressure) tank or more often refueling stops compared to liquid fuels, making it difficult to implement in heavy-duty or long-distance applications [9]. However, it emerges as a feasible technology for light- and medium-duty vehicles in the near future [10].

On spark-ignited (SI) engines, the use of hydrogen was reported as a substitute or combined with other fuels [11–14]. The main operating challenges of using pure hydrogen on SI engines with port-fuel injection (PFI) are back-fire and pre-ignition issues, mainly due to the contact of the fresh mixture with hot residual gases, hot spots and exhaust back-flow [15]. With the direct injection (DI) strategy, as the fuel is injected during the compression stroke, these phenomena are mitigated. Besides abnormal combustion prevention, the DI method also allows reaching higher engine load (above GDI operating condition), higher indicated efficiency at same load and air excess factor, and higher combustion velocity due to the turbulence induced by the fuel injection [11,16]. Hydrogen direct injection also allows working in stratified charge conditions extending the lean limit of a spark ignition engine [17]. In addition to the experimental studies, numerical studies investigated the flame front velocity [18], NO_X emissions and future emission regulation compliance [19–21].

On compression-ignited (CI) engines, experimental studies are reported using the hydrogen as the low reactivity fuel in the Dual-Fuel mode with diesel (high reactivity fuel), being able to reach up to 98% of the energy share ratio [22]. The hydrogen potential on CI engines was also assessed by numerical simulations, highlighting the challenges and future research topics to optimize the injection and combustion of gaseous fuel in this particular engine [23]. The hydrogen addition (up to 37.58% in energy basis) in diesel and diesel-vegetable oil mixtures was also experimentally assessed, pointing out the benefits of reducing HC, CO and CO_2 emission and specific fuel consumption, but with the drawbacks of lower thermal efficiency and higher NO_X emissions [24,25].

The use of hydrogen as a fuel is also reported on homogeneous charge compression ignition (HCCI) engines [26,27]. The high peak of heat release compels running at lean conditions, reducing the maximum power compared to the baseline diesel. Nevertheless, higher efficiency and lower pollutant emissions were reported.

Recent publications reported the use of pure hydrogen on SI ICE's [28–31], as well as the use of hydrogen to enable stable lean operation for various fuels, such as gasoline, compressed natural gas (CNG) and Acetone-Butanol-Ethanol (ABE) [32–34]. Due to its low ignition energy and high flame speed, the hydrogen addition reduces the cycle-to-cycle variability and extends the lean-burn limit. For this reason, pure hydrogen applications allow extremely high dilution rates with air or EGR, leading to very low NOx emissions at lean and ultra-lean mixtures while maintaining satisfactory combustion stability. The drawback, however, is the power limitation caused when a diluted operation strategy is used, limiting its use on high-density power demand applications.

Fischer et al. studied the use of hydrogen on a 1 L 3-cylinder turbocharged direct-injected gasoline engine converted to hydrogen operation. At 19 bar BMEP and stoichiometric condition, the hydrogen-fueled engine presented lower NOx emission and a faster and more stable combustion than gasoline, but with the inconvenience of a higher in-cylinder pressure and a

sharper pressure rise. The authors also highlight the potential of charge dilution (with air or EGR) to increase the indicated efficiency; limited, however, to the capability of the boost system to provide the required air/EGR rate. To conclude, the authors point out the inability of NOx reduction using lean operation above low part-load operation due to turbocharger capability issues, therefore being more suitable to use stoichiometric mixture in those conditions.

Bao et al. conducted experiments aiming achieve near-zero NOx emission at high power demand and high thermal efficiency on a 2 L 4-cylinder turbocharged direct-injected engine. As mentioned by the authors, the high injection pressure play an important role to achieve high engine load at mid-high engine speed while maintain low NOx emission. The better fuel homogenization caused by early injection it is also crucial to the NOx emission reduction. Additionally, the increase of the compression ratio and the use of a turbocharger allowed to significantly increase the engine load and brake thermal efficiency up to 13.3 bar BMEP and 40.4%, respectively, making it possible to achieve near-zero engine-out emission in most working conditions. Nevertheless, the authors remarks that it is impossible to achieve 20 bar BMEP or 42% of brake thermal efficiency without NOx penalization.

In addition to these experimental studies, recent papers reported a comprehensive review on the role of hydrogen for future internal combustion engines, which highlights the necessity of further contributions in such an interesting topic for the future mobility [35,36]. The current work, therefore, aims to investigate the hydrogen operating limits in a direct injection single-cylinder SI engine, identifying the leanest and richest mixture where a stable and safe operation is achieved. Afterwards, the hydrogen feasibility to replace conventional carbon-based fuels is assessed considering the engine performance, combustion parameters, exhaust gaseous emissions and indicated efficiency obtained with hydrogen and methane operation. To the best of the author's knowledge, there are few studies comparing the pure hydrogen operation with methane or compressed natural gas (CNG), furthermore these were carried out under non-similar test conditions such as low engine load or low injection pressure [37,38]. The main objective of comparing with methane, however, is to stablish a baseline case with a well-known and widely used fuel, which additionally was previously studied by the authors [39,40].

2. Materials and methods

This section describes the experimental facilities, fuel injection system and testing methodology used in this work.

2.1. Engine characteristics

The experimental investigation was carried out in a naturally aspirated 4-stroke single-cylinder SI engine. The cylinder head has a central sparkplug, four-valves and a pent-roof-shaped combustion chamber. Two injection systems are available in this engine: direct injection (DI) and port-fuel injection (PFI), but only DI configuration was used in this work. Table 1 summarizes the main characteristics of the engine.

Table 1. Engine specifications.

Engine type	4-stroke SI
Bore x Stroke [mm]	72 x 60
Displaced volume [cm^3]	244.3
Compression Ratio [-]	11.5:1
Injection system	DI @ 6.5 bar
SOI [CAD]	315 BTDC
Valve timing [CAD]	IVO=6 ATDC
	IVC=50 ABDC
	EVO=41 BBDC
	EVC=1 ATDC

Rated Power [kW]	16 @8000 rpm
Rated Torque [Nm]	20 @5500 rpm

2.2. Test cell characteristics

To allow proper engine monitoring and data acquisition of a wide range of relevant information for engine testing, the experimental activities were carried out in a fully instrumented test cell, as depicted in the scheme in Figure 1. The engine was coupled to an active dynamometer to control load and speed. The in-cylinder pressure was measured through an AVL GH12D piezoelectric pressure transducer in conjunction with an AVL FlexIFEM Piezo charge amplifier and referenced by an encoder with a resolution of 0.1 crank-angle degrees (CAD). A manifold absolute pressure (MAP) sensor was used to measure the intake pressure. The air and fuel mass flow rate were measured, respectively, through a Sensyflow NW 25 and a Brooks SLA5861 thermal mass flowmeters. A Bosch wide-band lambda sensor LSU 4.9, conditioned by an ETAS Lambda Meter LA4, determined the exhaust oxygen concentration and allowed the calculation of the actual air-to-fuel ratio. The ignition and injection settings were controlled by an AVL Engine Timing Unit (ETU) multi-channel system. All the sensors above were connected to an AVL IndiModul high-speed data acquisition unit, allowing real-time combustion analysis using AVL IndiCom software. Quantitative information about the combustion process and its cycle-to-cycle variability was obtained through a heat-release analysis from 400 consecutive cycles. A low-frequency system using type-K thermocouples was used to measure the intake and exhaust gas temperatures. The concentration of HC, CO, CO_2, O_2 and NOx on the exhaust were measured by an AVL DiGas 4000 gas analyzer.

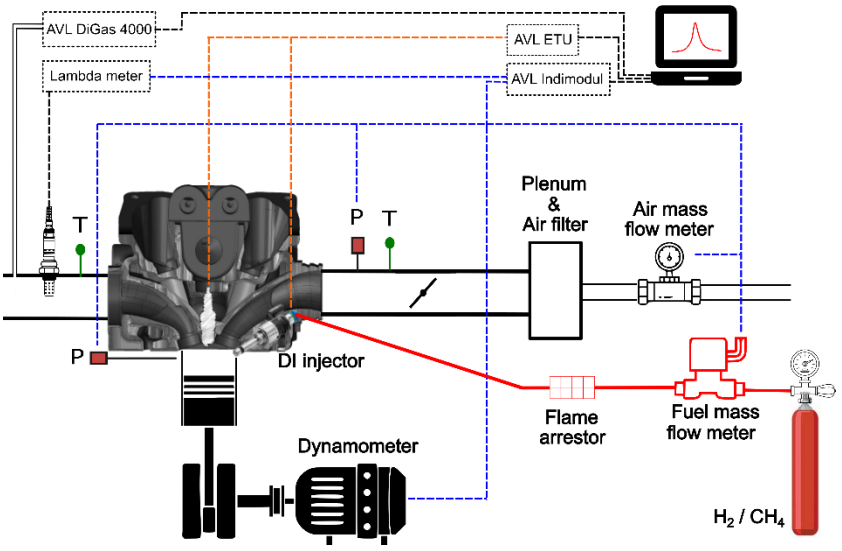

Figure 1 – Test cell scheme.

2.3. Fuel injection system

In this research, the engine was operated with methane (CH_4 ≥ 99.95 %) and gaseous hydrogen (H_2 ≥ 99.999%). Additional fuel characteristics are found in Table 2. Although the availability of PFI and DI injection strategies, the DI configuration was chosen due to the benefit of increasing the volumetric efficiency compared to the PFI, as related in further details on the author's previous works [41,42]. The DI configuration also helps prevent back-fire and pre-ignition phenomena, especially when fueled with hydrogen [15].

Table 2. Fuel characteristics. Source: [43,44]

Property	Methane	Hydrogen
Formula	CH_4	H_2
Lower Heating Value [MJ/kg]	50.0	120.0

Molecular weight [kg/kmol]	16.042	2.016
Density @ 300 K and 6.5 bar [kg/m^3]	4.2269	0.5233
Specific heat [kJ/kg K]	2.20	1.44
Ratio of specific ratio [-] @ 300 K and 6.5 bar	1.3198	1.4059
Gas constant [kJ/kg K]	0.5182	4.124
Autoignition temperature @ 1 atm and stoichiometric mixture [K]	813	858
Research Octane Number	120	120-140
Stoichiometric air/fuel ratio [kg/kg]	17.23	34.33

A natural gas low-pressure direct injector was adapted in the cylinder head and was used both for methane and hydrogen fuels. The upstream injector pressure was regulated at 6.5 bar (both for methane and hydrogen), ensuring critical flow through the nozzle. The start of injection (SOI) was set at 315 CAD-BTDC and the duration of injection (DOI) varied according to the desired operating condition (load and air-to-fuel ratio).

For safety reasons, the fuel gas line was equipped with a flame arrestor and a pneumatic-actuated valve downstream of the pressure regulator, enabling the operator to provide fuel gas to the injector only when the engine is powered, preventing premature wear and possible accidents due to the injector failures. The fuel gas line is then composed by the high-pressure fuel tank, pressure regulator, pneumatic-actuated valve, mass flow meter, flame arrestor and injector.

2.4. Hydrogen mass flow rate determination

Based on the mass rate of injection (i.e. fuel mass per energizing time curve) of a baseline gaseous fuel, it is possible to estimate the mass rate of injection of a different gaseous fuel using the physical properties of both fuels and the equation of a flow through an orifice of an ideal gas:

$$\frac{dm_{fuel}}{dt} = \frac{A_T P_{up}}{\sqrt{\gamma R T_o}} \gamma \left(\frac{2}{\gamma+1}\right)^{\frac{\gamma+1}{2(\gamma-1)}} \quad 2.1$$

where m_{fuel} is the mass of fuel, A_T is the cross-sectional area of the injector nozzle, P_{up} is the upstream injector gas pressure, γ is the ratio of specific heat, R is the gas constant, T_o is the upstream injector gas temperature.

In this work, the first approximation of hydrogen mass rate of injection was based on methane mass rate of injection. As the injector and the upstream thermodynamic condition are the same for both fuels, the difference in mass flow rate is only due to the different fuel physical properties. Therefore, assuming the pressure and temperature upstream of the injector as 6.5 bar and 300 K, respectively, the mass flow rate for hydrogen is 0.362 times the mass flow rate for methane at same duration of injection. Due to the linearity of the mass rate of injection and the supercritical flow condition of the injection process, the fuel mass injected of hydrogen can be determined for a wide range of DOI. Figure 2 shows the hydrogen mass flow rate versus energizing time for 2000 and 3000 rpm.

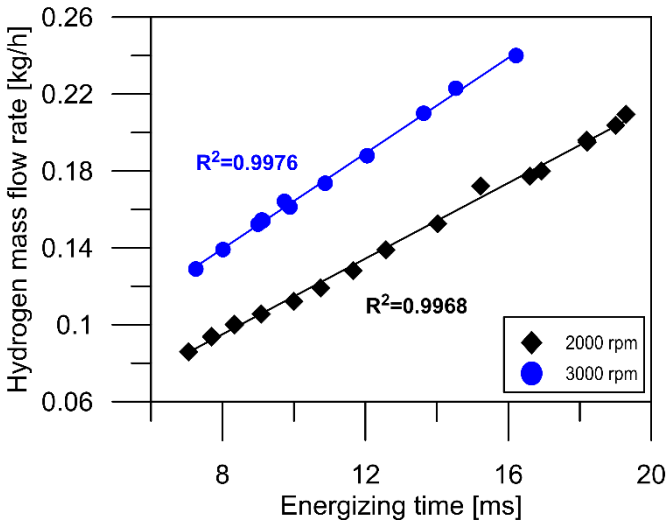

Figure 2 – Hydrogen mass flow rate versus energizing time.

2.5. Testing methodology

The present study is divided in two sections: (1) the first one explores the operating limits of a hydrogen fueled naturally-aspirated SI engine and (2) the second one performs a comparison between hydrogen and methane at 2000 and 3000 rpm at different engine loads and dilution rates.

2.5.1. Exploring the hydrogen operating limits

As a preliminary approach to identify the current limits with hydrogen fuel, the engine was operated from its lean limit to the closest-to-stoichiometric condition in lambda steps of 0.2. The former was constrained by the combustion stability ($IMEP_{COV}$ limit of 5%), whereas the latter by structural load (in-cylinder pressure and its rise rate). For each condition, the spark timing (ST) was adjusted at maximum brake-torque (MBT) timing, being this the only tuning parameter in each lambda value. Table 3 presents all the operating points for hydrogen fuel.

The objective during the operation with hydrogen was to explore the benefit of its wide flammability limits, de-throttling the engine and controlling the load by the amount of fuel injected. In this way, the pumping losses are diminished, and the NOx formation is greatly reduced due to the lower combustion temperature. At low loads, however, the cycle-to-cycle variability became excessively high due to the high dilution rate (lambda close to 3), suggesting that in such cases a throttled operation is needed.

Table 3. Engine test matrix for hydrogen operation.

Engine Speed [rpm]	Fuel	IMEP [bar]	$IMEP_{COV}$ [%]	TPS [%]	ST [CAD BTDC]	MFB50% [CAD ATDC]	DOI [CAD]	Lambda [-]
2000	Hydrogen	6.14	0.68	100.0	3.6	6.50	234	1.29
		5.72	0.71	100.0	4.6	6.85	220	1.39
		5.08	0.73	100.0	10	6.25	194	1.60
		4.72	0.88	100.0	8.6	8.05	168	1.81
		4.36	0.92	100.0	12.6	7.70	150	2.00
		4.13	0.97	100.0	14.6	8.70	139	2.20
		3.87	1.20	100.0	18.6	7.65	128	2.41
		3.66	1.45	100.0	20.6	9.60	119	2.60

		3.44	1.50	100.0	24.6	10.45	109	2.80
		3.21	2.01	100.0	26.6	11.65	100	3.01
		2.97	2.83	100.0	28.6	13.50	92	3.18
		2.46	6.63	100.0	28.6	18.40	84	3.40
3000	Hydrogen	5.50	0.84	100.0	13.8	7.75	295	1.97
		5.09	0.78	100.0	16.8	7.10	265	2.20
		4.76	0.76	100.0	18.8	7.05	248	2.41
		4.32	0.94	100.0	20.8	9.10	215	2.59
		4.02	0.87	100.0	23	9.65	194	2.78
		3.69	1.04	100.0	24.8	10.80	176	3.01
		3.41	1.80	100.0	27	12.00	162	3.20
		3.00	3.06	100.0	27	15.00	144	3.40
		2.48	6.78	100.0	27	17.75	130	3.51

2.5.2.Hydrogen potential to replace methane as fuel

In the second phase of the study, a comparison between hydrogen and methane was performed at 2000 and 3000 rpm at different engine loads and dilution rates. The engine performance, combustion parameters, indicated efficiency and exhaust emissions of both fuels are compared and discussed. For each condition, the spark timing (ST) was adjusted at MBT timing. The operating conditions used in the comparison are described in Table 4.

While using hydrogen the engine was operated at wide-open throttle (WOT), with methane, nonetheless, the throttled operation was necessary to limit the load and maintain the dilution rate within admissible levels to a proper combustion development. Moreover, due to a narrow flammability range of the methane and knock limitation on close to stoichiometric mixtures with hydrogen (further detailed on Section 3.1), it was impossible to make a comparison at same dilution rate between both fuels. Therefore, the methodology chosen for the methane operation was to reproduce the same IMEP range as the hydrogen, preserving the stoichiometric mixture to ensure a good conversion efficiency of the three-way catalyst (TWC).

Table 4. Engine test matrix for methane operation, λ=1.

Engine Speed [rpm]	Fuel	IMEP [bar]	$IMEP_{COV}$ [%]	ST [CAD BTDC]	MFB50% [CAD ATDC]	DOI [CAD]
2000	Methane	5.42	0.7	28	8.2	150
		5.15	0.9	28	10.3	140
		4.43	1.8	34	9.7	125
		4.31	3.7	28	18.1	118
		4.14	1.4	34	11.4	114
		3.71	6.3	34	17.0	105
		2.59	15.4	38	27.4	86
3000	Methane	5.64	2.27	31	12.6	243
		4.86	1.7	34	11.2	200
		4.16	2.0	36	8.9	180
		3.23	1.9	44	9.9	136
		2.71	5.5	39	18.0	120

		2.29	3.4	51	9.9	100

3. Results and discussion

3.1. Exploring the hydrogen operating limits

The first step during the experimental campaign with hydrogen was to sweep the mixture dilution and optimize the ST to achieve MBT on each operating point. It is important to notice that only WOT conditions were assessed during this exploratory campaign; therefore, the load was controlled by the amount of injected fuel. Due to the lean operation, a substantial engine power reduction was noticed when fueled with hydrogen. The maximum IMEP reached was 6.14 bar, about 53% of the maximum rated engine load. To overcome this power limitation while maintaining a diluted mixture, a supercharged operation is recommended for future works.

As depicted in Figure 3, as the mixture dilution is increased, the combustion stability (quantified by the coefficient of variation of the Indicated Mean Effective Pressure – $IMEP_{COV}$) is worsened. This exacerbated cycle-to-cycle variability in reason of the mixture composition is caused by the deterioration of the flame development on its initial stages, leading to different combustion development or, in some cases, flame front quenching. The condition in which the $IMEP_{COV}$ limit of 5% has been exceeded was lambda 3.40 and 3.51 at 2000 and 3000 rpm, respectively. Therefore, at low engine loads, where the dilution increases at WOT condition, a throttled operation is recommended to reduce the mixture dilution and stabilize the combustion. This partialization reduces the high cycle-to-cycle variability and misfire occurrences that penalized the engine efficiency and would affect the drivability in a future vehicle application. For this particular engine, setting a $IMEP_{COV}$ limit of 5%, the leanest possible mixture would be around lambda 3.31 and 3.46 for 2000 and 3000 rpm, respectively.

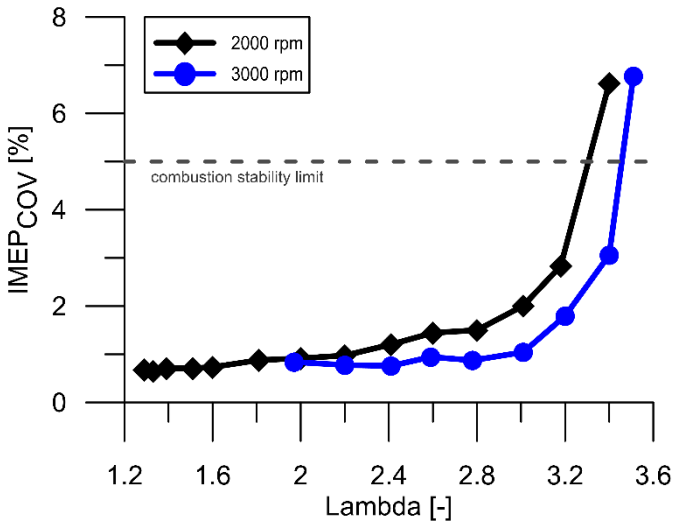

Figure 3 – Coefficient of variation of the IMEP in 400 consecutive cycles.

As the engine load increases (here represented by the dilution rate due to the WOT condition), the in-cylinder pressure and temperature become higher, which increase the end-gas temperature and promotes the formation of hotspots in the combustion chamber, increasing the tendency to knock in such conditions. In this study, the engine knock was monitored by the maximum amplitude of pressure oscillations (MAPO), where a band-pass filter (between 5 and 20 KHz) is applied to the in-cylinder pressure and the maximum amplitude of the high-frequency resulting signal is taken. Due to the random occurrence of the knock, the MAPO was calculated for each individual cycle and the mean value over 400 cycles represents the frequency and intensity of this abnormal event. As the MAPO is a parameter based on the pressure wave caused by the knock phenomenon, it depends on the geometry of the combustion chamber and must be empirically determined for each engine geometry and speed. Since no knock condition was detected, it was not possible to define the MAPO limits for hydrogen operation on the tested conditions. However, under MAPO 0.23 and 0.21 bar, for 2000 and 3000 rpm respectively, knock-safe conditions are obtained thanks to the hydrogen direct injection and the relatively low load

due to naturally-aspirated intake system. The MAPO values for all tested conditions can be observed on Figure 4.

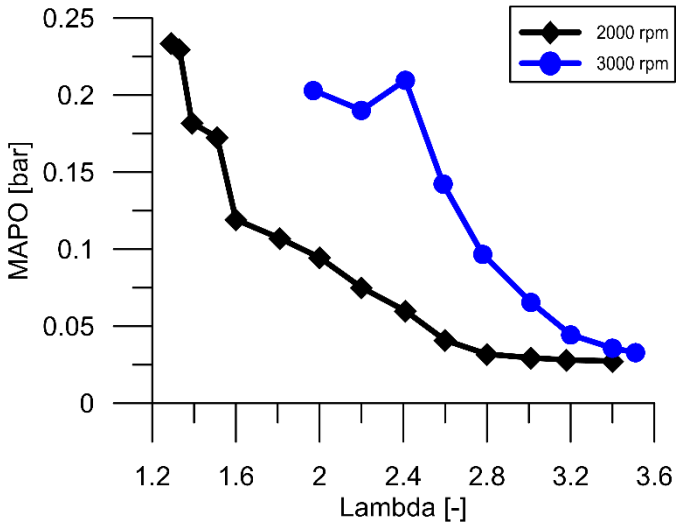

Figure 4 – Mean of maximum MAPO in 400 consecutive cycles.

Figure 5 shows the mean of the maximum pressure rise rate for a wide range of mixture dilution and the two tested engine speeds. It can be observed that higher hydrogen concentrations lead to higher in-cylinder pressure rise rates, an expected behavior since the energy delivered by the fuel is gradually increased. Nonetheless, excessively high (5 bar/cad) in-cylinder pressure rise rates were obtained when approaching stoichiometric mixtures, therefore the engine has not been tested on conditions with mixtures richer than lambda 1.3 at 2000 rpm to avoid structural damages.

For higher engine speed cases, at 3000 rpm, even though the maximum pressure rise rate was adequate, the injector was unable to supply the fuel demand necessary to reach lambda values below 2.0. The reason is the combination of a shorter available injection time (in seconds) due to higher engine speed, low density of the hydrogen (one-eighth of methane density) and the use of low-pressure direct injection, which limits the end of injection to a given point that the in-cylinder pressure is below the injection pressure (here established at 65 CAD-BTDC). For this limited condition (lambda 2.0 at 3000 rpm), the DOI was changed from 315 to 355 CAD-BTDC to increase the available injection time, however a worse cylinder filling was noticed due to an overlap with the intake process, causing a lower in-cylinder pressure during compression stroke as shown in Figure 6.

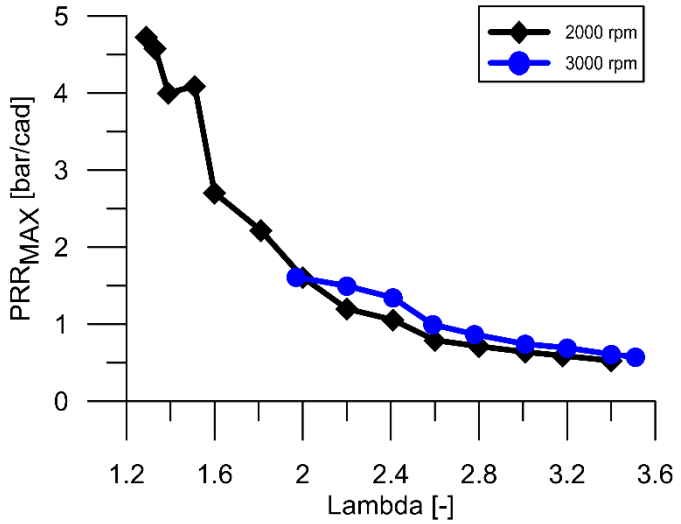

Figure 5 – Mean of maximum pressure rise rate in 400 consecutive cycles.

Based on the crank angle resolved in-cylinder pressure, a heat-released analysis was carried out to obtain quantitative combustion parameters such as the rate of heat released (RoHR), and the mass fraction burned profile. The in-cylinder pressure traces and the RoHR for a wide range of mixture dilution are depicted in Figure 6, at 2000 rpm on the left-hand and 3000 rpm on the right-hand. As expected, the maximum in-cylinder pressure and the peak of rate of heat released decrease as the mixture is leaned. This behavior is due to the lower amount of fuel injected and the slower flame speed caused by the air dilution, which enlarge the combustion duration and slow down the energy release.

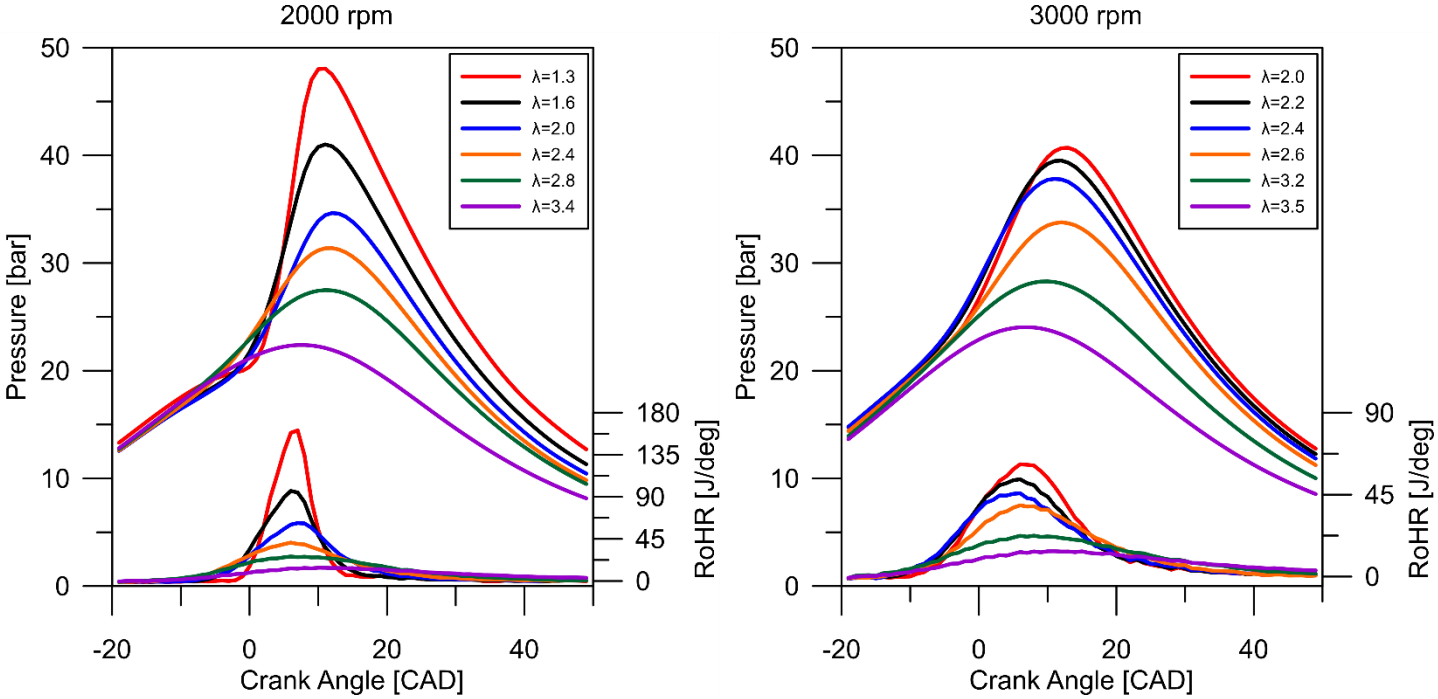

Figure 6 – Effect of charge dilution on the mean of in-cylinder pressure and rate of heat released at 2000 rpm (left) and 3000 rpm (right).

The slower combustion also requires more advanced spark timings to ensure a proper combustion centering, characterized by the crank angle at which 50% of the mixture is burned (MFB50%). The evolution of the spark timing necessary to achieve MFB50% around 8 CAD-ATDC for each mixture composition tested at 2000 rpm is depicted on Figure 7. As can be seen, the spark timing has to be advanced as the mixture is leaned. However, for mixtures leaner than lambda 2.8, the combustion duration is so extended that the spark timing necessary to center the combustion ends up moving the maximum in-cylinder pressure towards TDC, lowering the indicated efficiency. At very lean mixtures (e.g. lambda 3.0 and beyond), there is a complete mismatch between these two engine calibration criteria, indicating that a faster combustion is necessary. In this sense, the pre-chamber ignition concept could be an effective method to shorten the combustion duration and it could enable the use of very lean mixtures, especially the configuration that uses stoichiometric mixture inside the pre-chamber, called active configuration.

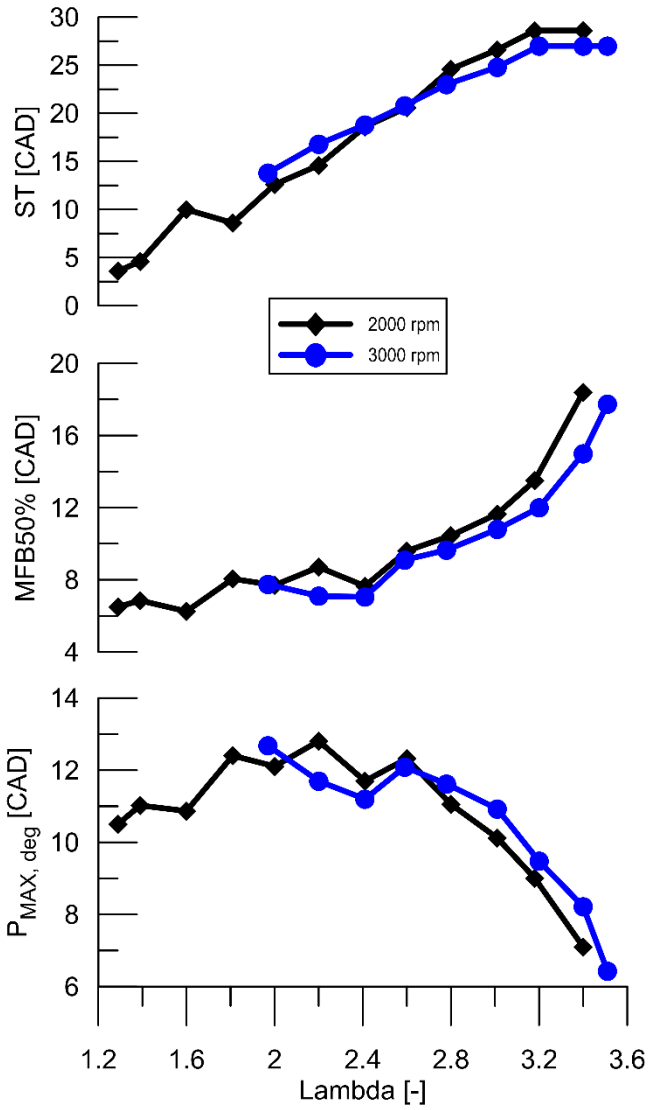

Figure 7 – Effect of charge dilution on combustion centering.

In terms of exhaust gaseous emissions, Figure 8 shows how the formation of nitrous oxide (NO_X) is greatly reduced as the air dilution ratio is increased, reaching zero emission at lambda 2.2 and 3.0 at 2000 and 3000 rpm, respectively. As the NOx formation rate is strongly dependent on the in-cylinder temperature, the operating conditions close to stoichiometric mixtures presents the higher NOx emissions precisely due to the higher in-cylinder temperature, as depicted on Figure 9. Another point to be remarked by observing Figure 8 and Figure 9 is that the higher engine speed presents the higher NOx emission at the same lambda; this is due to the higher in-cylinder temperature explained by the lower heat losses to the walls. In addition to temperature, the oxygen concentration plays an important role on the NOx formation, nevertheless as all tested conditions are at lean operation, this was not crucial in the present work.

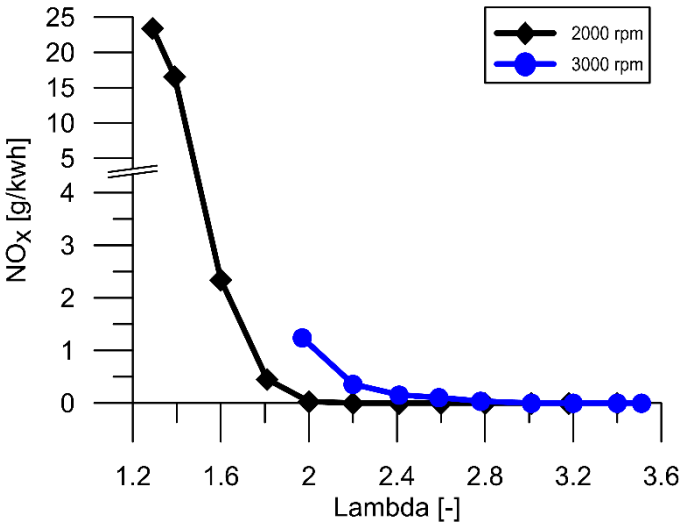

Figure 8 – Effect of charge dilution on engine-out NOx emission.

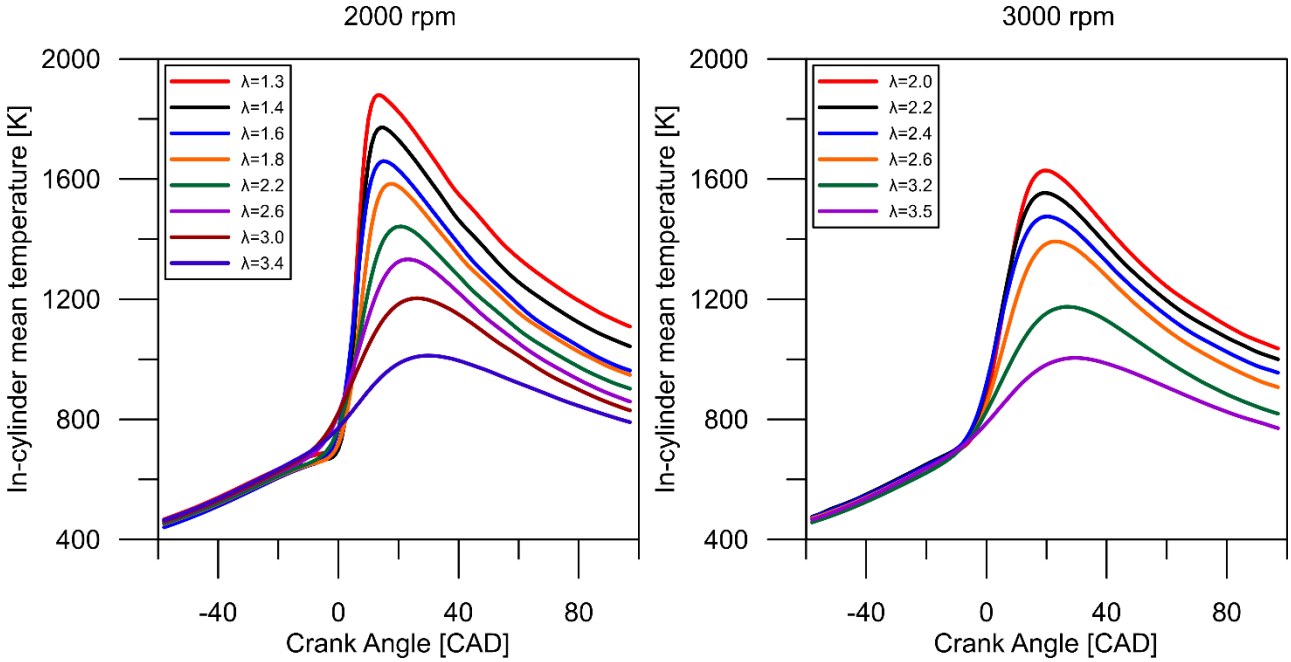

Figure 9 – In-cylinder mean temperature crank angle evolution for different charge dilution levels at 2000 rpm (left) and 3000 rpm (right).

As hydrogen is a carbon-free fuel, zero CO emissions and very low amounts of HC were detected both for 2000 and 3000 rpm for all operation conditions tested. It is worthy to mention that small amounts of HC are usually due to the presence of lubricant film on chamber walls.

3.2. Hydrogen potential to replace methane as fuel

This section presents an assessment of the potential of the hydrogen to replace conventional fuels on SI engines, such as methane. Engine performance, combustion parameters, indicated efficiency and exhaust gaseous emissions of the hydrogen operation were compared with a methane operation at equivalent engine load. The main benefits of replacing methane with hydrogen are the possibility to de-throttle the engine to reduce the pumping losses, and the suitable flame front velocity even at lean operation. Besides, the lean operation also increases the gas specific heat ratio and decreases the average burned-gas temperature, leading to a higher expansion work and lower heat losses to the combustion chamber walls. Therefore, these advantages suggesting a higher indicated efficiency with hydrogen from a thermodynamic and operational point of view will be fully assessed and discussed.

In a naturally aspirated engine, to achieve a greater indicated efficiency it is desirable that the energy lost during the intake and exhaust strokes be as small as possible. For both hydrogen and methane operation it was quantified by the pumping mean effective pressure (PMEP), represented in Figure 10. As it can be seen, the pumping losses with hydrogen operation represent 28% and 47% of the methane operation at 2000 and 3000 rpm, respectively. Thus, combining hydrogen and de-throttling operation, less fuel-energy is necessary to achieve the same indicated work (thanks to the lower energy spent during the gas exchange process), resulting in a gain in indicated efficiency.

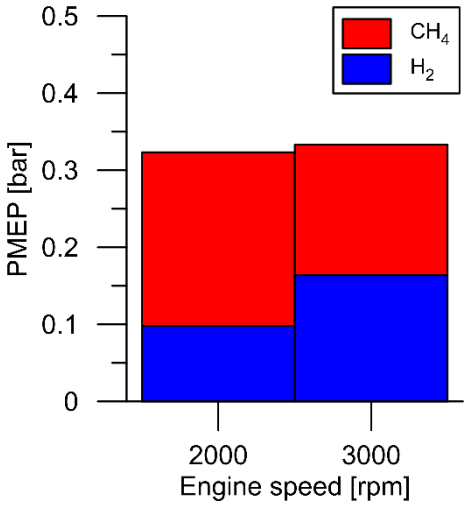

Figure 10 – PMEP at 2000 and 3000 rpm at equivalent IMEP for hydrogen and methane.

Besides the pumping losses, the combustion duration also plays an important role in the indicated efficiency, where a faster combustion leads to a higher indicated efficiency due to its approximation to a constant-volume ideal cycle. In this sense, Figure 11 presents the rate of heat released for methane and hydrogen at 2000 rpm and equivalent engine load, normalized by the maximum hydrogen value. It can be said that even with a leaner mixture (lambda 2.0 vs lambda 1.0), the hydrogen presented a faster combustion and a higher peak of heat released, contributing to a higher indicated efficiency.

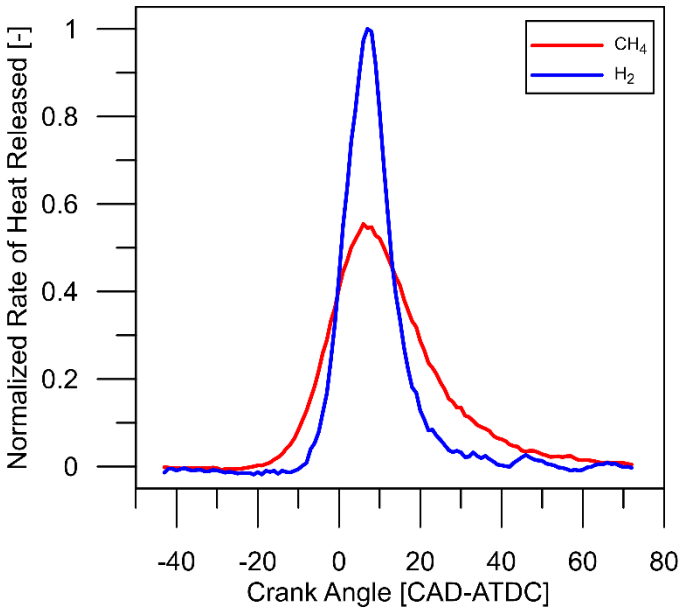

Figure 11 – Normalized rate of heat released. IMEP 4.3 bar @ 2000 rpm

Figure 12 shows the engine-out indicated specific NOx emissions for hydrogen and methane at 2000 and 3000 rpm. As can be seen, the engine emitted less NOx when fueled with hydrogen

for the most part of the tested conditions, especially below IMEP 4.5 where no NOx emissions were measured for hydrogen. As the engine load is increased, both fuels presented higher NOx formation due to the higher in-cylinder temperature. However, the higher oxygen concentration in hydrogen operation contributed to a higher NOx emission in the last tested load range, as observed at 2000 rpm and IMEP 5.7, where the hydrogen NOx emissions are higher than methane.

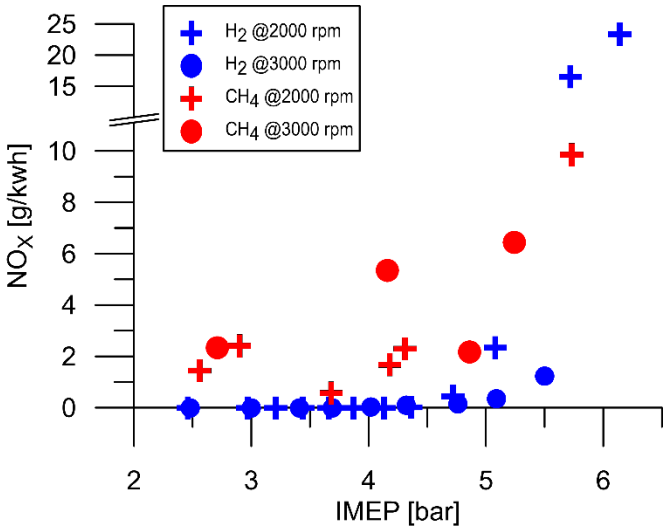

Figure 12 – Engine-out indicated specific NOx emission for all tested conditions.

The indicated specific HC and CO emissions for all operating points are shown in Figure 13 and Figure 14, respectively. As expected, the hydrogen presented lower HC and CO emissions than methane as a result of the absence of carbon on its composition. The small amount of HC emission on hydrogen operation can be related to the contamination caused by the thin layer of lubricant oil on the cylinder walls.

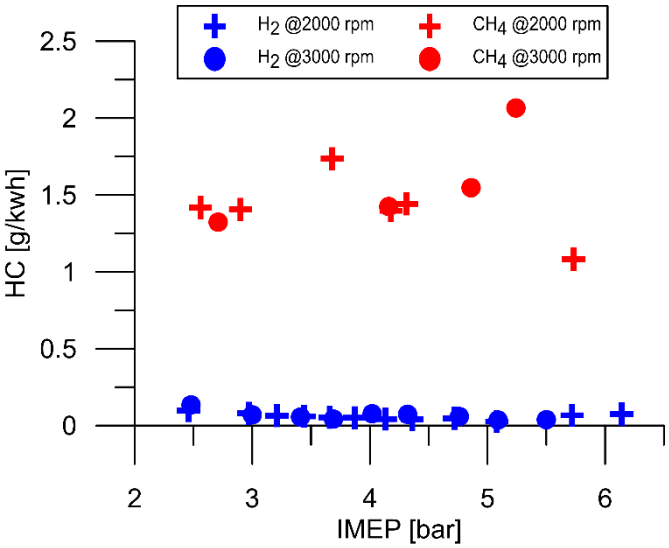

Figure 13 – Engine-out indicated specific HC emission for all tested conditions.

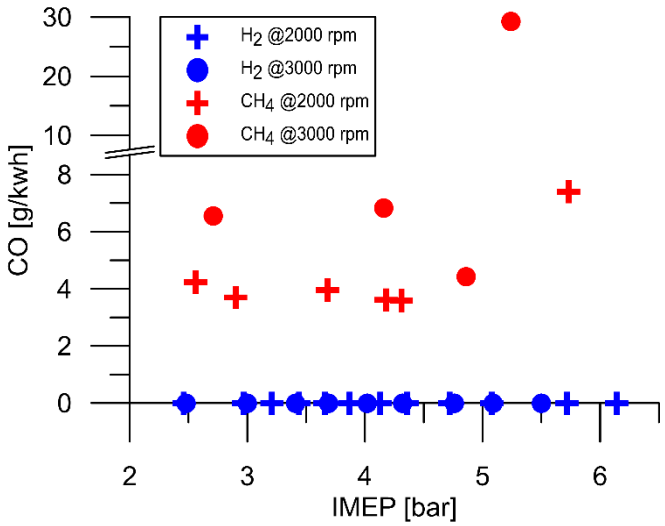

Figure 14 – Engine-out indicated specific CO emission for all tested conditions.

Finally, to support all the reasoning done throughout this section, the indicated efficiency for hydrogen and methane operation at 2000 and 3000 rpm and different engine load are presented in Figure 15. The hydrogen, therefore, showed a substantial gain both at 2000 rpm and 3000 rpm for all tested range of engine load. The highest hydrogen indicated efficiency (42.4%) was obtained at 3000 rpm and 5.5 bar IMEP, which represents a gain of 8.6% in comparison with methane at similar engine load.

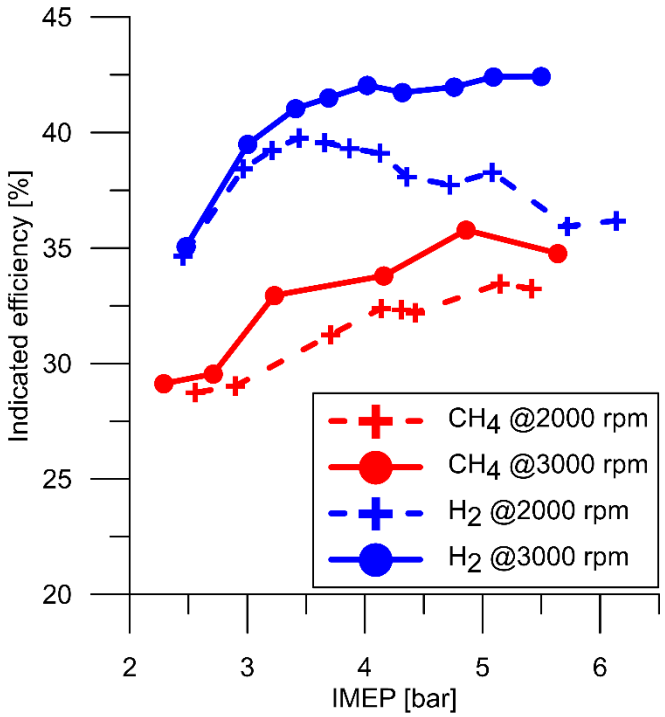

Figure 15 –Indicated efficiency comparison between hydrogen and methane for all tested conditions.

4. Conclusions

In this work an experimental investigation of the operating limits of a single cylinder naturally-aspirated SI engine fueled with hydrogen is presented and discussed. Its performance, combustion parameters, exhaust emissions and indicated efficiency were then compared to methane under similar engine load conditions. The following main conclusions can be deduced from this study:

- Fueled with hydrogen, the engine could be operated from lambda 1.3 up to 3.4 at 2000 rpm. The closer-to-stoichiometric mixture was limited by the abrupt in-cylinder pressure rise (approaching 5 bar/cad), whereas the combustion stability constrained the most diluted one (exceeding 5% of covariance on IMEP). For 3000 rpm, the lean limit was reached at lambda 3.5 and the injector capacity limited the mixture composition at lambda 2.0.
- The direct injection fuel system ensured knock-safe operation for all tested conditions (up to 6.14 bar IMEP @2000 rpm).
- Throttled operation is recommended at low engine loads to decrease the mixture dilution and reduce the cycle-to-cycle variability.
- To overcome the power limitation imposed by the diluted mixture, a supercharged operation (with a turbocharger or a mechanical supercharger) is recommended for futures works.
- Despite its mostly higher laminar flame speed, the hydrogen combustion at high dilution rates (especially leaner than lambda 2.8) was not fast enough to center the combustion (MFB50%) around 8 CAD-ATDC, resulting in low indicated efficiency in such conditions. Alternative combustion methods that shorten the combustion duration (e.g. pre-chamber ignition concept) may extend the current lean limit achieved with conventional sparkplug.
- In comparison with methane, the engine fueled with hydrogen presented lower pumping losses on all tested operating points thanks to the un-throttled operation.
- Even with diluted mixture, the hydrogen presented a faster combustion than methane, which contributed to a higher indicated efficiency.
- The absence of carbon molecules contributed to lower engine-out HC and CO emissions of hydrogen in comparison with methane. Moreover, the hydrogen NOx emissions were lower at most operating points thanks to the lean operation.
- The hydrogen showed a substantial gain in indicated efficiency in comparison with methane both at 2000 rpm and 3000 rpm for all tested range of engine load.

To conclude, hydrogen proved to be a promising carbon-free fuel to replace the conventional fuels currently used on SI engines.

Acknowledgments

The authors would like to thank different members of the Istituto di Scienze e Tecnologie per l'Energia e la Mobilità Sostenibili (Consiglio Nazionale delle Ricerche) and CMT- Motores Térmicos (Universitat Politècnica de València), directly or indirectly involved in this work, for their contribution to this work. In particular, the authors are grateful to Mr. Bruno Sgammato and Mr. Carlo Rossi for their precious technical support. The authors also thank the Universitat Politècnica de València for the mobility grant given to Jácson Beltrão de Vargas Antolini.

References

[1] Huang J, Pan X, Guo X, Li G. Impacts of air pollution wave on years of life lost: A crucial way to communicate the health risks of air pollution to the public. Environ Int 2018;113:42–9. https://doi.org/10.1016/j.envint.2018.01.022.

[2] European Union. Regulation (EU) 2017/631 of the European Parliament and of the Council. Off J Eur Union 2017;L 168:71.

[3] Reitz RD, Ogawa H, Payri R, Fansler T, Kokjohn S, Moriyoshi Y, et al. IJER editorial: The future of the internal combustion engine. Int J Engine Res 2020;21:3–10. https://doi.org/10.1177/1468087419877990.

[4] Squaiella LLF, Martins CA, Lacava PT. Strategies for emission control in diesel engine to meet Euro VI. Fuel 2013;104:183–93. https://doi.org/10.1016/j.fuel.2012.07.027.

[5] Ugurlu A. An emission analysis study of hydrogen powered vehicles. Int J Hydrogen Energy 2020;45:26522–35. https://doi.org/10.1016/j.ijhydene.2020.05.156.

[6] Martinez-Burgos WJ, de Souza Candeo E, Pedroni Medeiros AB, Cesar de Carvalho J, Oliveira de Andrade Tanobe V, Soccol CR, et al. Hydrogen: Current advances and patented technologies of its renewable production. J Clean Prod 2021;286:124970.

https://doi.org/10.1016/j.jclepro.2020.124970.

[7] Hosseini SE, Wahid MA. Hydrogen production from renewable and sustainable energy resources: Promising green energy carrier for clean development. Renew Sustain Energy Rev 2016;57:850–66. https://doi.org/10.1016/j.rser.2015.12.112.

[8] Shadidi B, Najafi G, Yusaf T. A Review of Hydrogen as a Fuel in Internal Combustion Engines. Energies 2021;14:6209. https://doi.org/10.3390/en14196209.

[9] Nugroho R, Rose PK, Gnann T, Wei M. Cost of a potential hydrogen-refueling network for heavy-duty vehicles with long-haul application in Germany 2050. Int J Hydrogen Energy 2021;46:35459–78. https://doi.org/10.1016/j.ijhydene.2021.08.088.

[10] Verhelst S, Wallner T. Hydrogen-fueled internal combustion engines. Prog Energy Combust Sci 2009;35:490–527. https://doi.org/10.1016/j.pecs.2009.08.001.

[11] Berckmüller M, Rottengruber H, Eder A, Brehm N, Elsässer G, Müller-Alander G, et al. Potentials of a charged SI-hydrogen engine. SAE Tech Pap 2003;2003. https://doi.org/10.4271/2003-01-3210.

[12] Zhang R, Chen L, Wei H, Pan J, Li J, Yang P, et al. Optical study on the effects of the hydrogen injection timing on lean combustion characteristics using a natural gas/hydrogen dual-fuel injected spark-ignition engine. Int J Hydrogen Energy 2021;46:20777–89. https://doi.org/10.1016/j.ijhydene.2021.03.171.

[13] Mohammadi A, Shioji M, Nakai Y, Ishikura W, Tabo E. Performance and combustion characteristics of a direct injection SI hydrogen engine. Int J Hydrogen Energy 2007;32:296–304. https://doi.org/10.1016/j.ijhydene.2006.06.005.

[14] Lhuillier C, Brequigny P, Contino F, Mounaïm-Rousselle C. Experimental study on ammonia/hydrogen/air combustion in spark ignition engine conditions. Fuel 2020;269:117448. https://doi.org/10.1016/j.fuel.2020.117448.

[15] Gao J, Wang X, Song P, Tian G, Ma C. Review of the backfire occurrences and control strategies for port hydrogen injection internal combustion engines. Fuel 2022;307:121553. https://doi.org/10.1016/j.fuel.2021.121553.

[16] Thawko A, Persy SA, Eyal A, Tartakovsky L. Effects of Fuel Injection Method on Energy Efficiency and Combustion Characteristics of SI Engine Fed with a Hydrogen-Rich Reformate. SAE Tech Pap 2020:1–12. https://doi.org/10.4271/2020-01-2082.

[17] Lee S, Kim G, Bae C. Effect of injection and ignition timing on a hydrogen-lean stratified charge combustion engine. Int J Engine Res 2021. https://doi.org/10.1177/14680874211034682.

[18] Iafrate N, Matrat M, Zaccardi JM. Numerical investigations on hydrogen-enhanced combustion in ultra-lean gasoline spark-ignition engines. Int J Engine Res 2021;22:375–89. https://doi.org/10.1177/1468087419870688.

[19] Chaurasia S, Sreedhara S, Duvvuri PP. Combustion Characteristics of Premixed Hydrogen Fueled Spark Ignition Engine. Bull JSAE, 2021, p. 1–10. https://doi.org/10.4271/2021-26-0224.

[20] Rezaei R, Kovacs D, Hayduk C, Mennig M, Delebinski T. Euro VII and Beyond with Hydrogen Combustion for Commercial Vehicle Applications: From Concept to Series Development. SAE Tech Pap Ser 2021;1:1–11. https://doi.org/10.4271/2021-01-1196.

[21] Wallner T, Matthias NS, Scarcelli R, Kwon JC. Evaluation of the efficiency and the drive cycle emissions for a hydrogen direct-injection engine. Proc Inst Mech Eng Part D J Automob Eng 2013;227:99–109. https://doi.org/10.1177/0954407012461875.

[22] Dimitriou P, Kumar M, Tsujimura T, Suzuki Y. Combustion and emission characteristics of a hydrogen-diesel dual-fuel engine. Int J Hydrogen Energy 2018;43:13605–17. https://doi.org/10.1016/j.ijhydene.2018.05.062.

[23] Babayev R, Andersson A, Serra Dalmau A, Im HG, Johansson B. Computational comparison of the conventional diesel and hydrogen direct-injection compression-ignition

combustion engines. Fuel 2022;307:121909. https://doi.org/10.1016/j.fuel.2021.121909.

[24] Rocha HMZ, Nogueira MFM, Guerra DR da S, Hernández JJ, Queiroz LS. Improving the usage of vegetable oils in generator sets used for off-grid power generation by hydrogen addition. Int J Hydrogen Energy 2021;46:35479–94. https://doi.org/10.1016/j.ijhydene.2021.08.094.

[25] YILMAZ IT. The effect of hydrogen on the thermal efficiency and combustion process of the low compression ratio CI engine. Appl Therm Eng 2021;197:117381. https://doi.org/10.1016/j.applthermaleng.2021.117381.

[26] Gomes Antunes JM, Mikalsen R, Roskilly AP. An investigation of hydrogen-fuelled HCCI engine performance and operation. Int J Hydrogen Energy 2008;33:5823–8. https://doi.org/10.1016/j.ijhydene.2008.07.121.

[27] Mohamed Ibrahim M, Ramesh A. Investigations on the effects of intake temperature and charge dilution in a hydrogen fueled HCCI engine. Int J Hydrogen Energy 2014;39:14097–108. https://doi.org/10.1016/j.ijhydene.2014.07.019.

[28] Fischer M, Sterlepper S, Pischinger S, Seibel J, Kramer U, Lorenz T. Operation principles for hydrogen spark ignited direct injection engines for passenger car applications. Int J Hydrogen Energy 2022;47:5638–49. https://doi.org/10.1016/j.ijhydene.2021.11.134.

[29] Oikawa M, Kojiya Y, Sato R, Goma K, Takagi Y, Mihara Y. Effect of supercharging on improving thermal efficiency and modifying combustion characteristics in lean-burn direct-injection near-zero-emission hydrogen engines. Int J Hydrogen Energy 2022;47:1319–27. https://doi.org/10.1016/j.ijhydene.2021.10.061.

[30] Bao L zhi, Sun B gang, Luo Q he. Experimental investigation of the achieving methods and the working characteristics of a near-zero NOx emission turbocharged direct-injection hydrogen engine. Fuel 2022;319:123746. https://doi.org/10.1016/j.fuel.2022.123746.

[31] Gürbüz H, Akçay İH. Evaluating the effects of boosting intake-air pressure on the performance and environmental-economic indicators in a hydrogen-fueled SI engine. Int J Hydrogen Energy 2021;46:28801–10. https://doi.org/10.1016/j.ijhydene.2021.06.099.

[32] Niu R, Yu X, Du Y, Xie H, Wu H, Sun Y. Effect of hydrogen proportion on lean burn performance of a dual fuel SI engine using hydrogen direct-injection. Fuel 2016;186:792–9. https://doi.org/10.1016/j.fuel.2016.09.021.

[33] Molina S, Novella R, Gomez-Soriano J, Olcina-Girona M. Experimental Evaluation of Methane-Hydrogen Mixtures for Enabling Stable Lean Combustion in Spark-Ignition Engines for Automotive Applications. SAE Tech Pap Ser 2022;1:1–12. https://doi.org/10.4271/2022-01-0471.

[34] Yu X, Li D, Yang S, Sun P, Guo Z, Yang H, et al. Effects of hydrogen direct injection on combustion and emission characteristics of a hydrogen/Acetone-Butanol-Ethanol dual-fuel spark ignition engine under lean-burn conditions. Int J Hydrogen Energy 2020;45:34193–203. https://doi.org/10.1016/j.ijhydene.2020.09.080.

[35] Stępień Z. A comprehensive overview of hydrogen-fueled internal combustion engines: Achievements and future challenges. Energies 2021;14. https://doi.org/10.3390/en14206504.

[36] Onorati A, Payri R, Vaglieco B, Agarwal A, Bae C, Bruneaux G, et al. The role of hydrogen for future internal combustion engines. Int J Engine Res 2022;23:529–40. https://doi.org/10.1177/14680874221081947.

[37] Sagar SMV, Agarwal AK. Experimental investigation of varying composition of HCNG on performance and combustion characteristics of a SI engine. Int J Hydrogen Energy 2017;42:13234–44. https://doi.org/10.1016/j.ijhydene.2017.03.063.

[38] Das LM, Gulati R, Gupta PK. Comparative evaluation of the performance characteristics of a spark ignition engine using hydrogen and compressed natural gas as alternative fuels. Int J Hydrogen Energy 2000;25:783–93. https://doi.org/10.1016/S0360-3199(99)00103-2.

[39] Di Iorio S, Sementa P, Vaglieco BM. Analysis of combustion of methane and hydrogen–methane blends in small DI SI (direct injection spark ignition) engine using advanced diagnostics. Energy 2016;108:99–107. https://doi.org/10.1016/j.energy.2015.09.012.

[40] Catapano F, Di Iorio S, Sementa P, Vaglieco BM. Particle Formation and Emissions in an Optical Small Displacement SI Engine Dual Fueled with CNG di and Gasoline PFI. SAE Tech Pap 2017;2017-September. https://doi.org/10.4271/2017-24-0092.

[41] Catapano F, Di Iorio S, Sementa P, Vaglieco BM. Analysis of energy efficiency of methane and hydrogen-methane blends in a PFI/DI SI research engine. Energy 2016;117:378–87. https://doi.org/10.1016/j.energy.2016.06.043.

[42] Catapano F, Iorio S Di, Sementa P, Vaglieco BM. Optimization of the compressed natural gas direct injection in a small research spark ignition engine. Int J Engine Res 2017;18:118–30. https://doi.org/10.1177/1468087417692505.

[43] Lemmon EW, McLinden MO, Friend DG. Thermophysical Properties of Fluid Systems. In: Linstrom PJ, Mallard WG, editors. NIST Chem. Webb., Gaithersburg MD: National Institute of Standards and Technology; n.d. https://doi.org/https://doi.org/10.18434/T4D303.

[44] Heywoood JB. Internal Combustion Engine Fundamentals. Second. New York, N.Y.: McGraw Hill; 2018.

Notations

ABE	Acetone-Butanol-Ethanol
ATDC	After top dead center
ABDC	After bottom dead center
BDC	Bottom dead center
BTE	Brake thermal efficiency
CAD	Crank angle degree
CI	Compression ignition
CNG	Compressed natural gas
CO	Carbon monoxide
CO_2	Carbon dioxide
DI	Direct injection
DOI	Duration of injection
EGR	Exhaust gas recirculation
ETU	Engine timing unit
GDI	Gasoline direct injection
HC	Hydrocarbon
ICE	Internal combustion engine
IMEP	Indicated mean effective pressure
MAPO	Maximum amplitude of pressure oscillations
MBT	Maximum brake-torque
MFB	Mass fraction burned
m_{fuel}	Mass of fuel injected
NOx	Nitrous oxide
P_{up}	Upstream injector gas pressure
PFI	Port fuel injection
PMEP	Pumping mean effective pressure
RoHR	Rate of heat released
R	Gas constant
SI	Spark ignition
SOI	Start of injection
ST	Spark timing
T_o	Upstream injector gas temperature
TDC	Top dead center
WOT	Wide-open throttle
WTW	Well-to-wheel

Greek letters

γ	Specific heat ratio c_p/c_v

λ	Relative air/fuel ratio